Fermi National Accelerator Laboratory

FERMILAB-Pub-96/188-E
E683

The Emergence of Jet Dominance in γ-p Interactions at Fixed-Target Energies

D. Alton et al.
The E683 Collaboration
Fermi National Accelerator Laboratory
P.O. Box 500, Batavia, Illinois 60510

October 1996

Submitted to *Physical Review Letters*

Operated by Universities Research Association Inc. under Contract No. DE-AC02-76CHO3000 with the United States Department of Energy

Disclaimer

Distribution

FERMILAB Pub-96/188-E

The Emergence of Jet Dominance in γ-p Interactions at Fixed-Target Energies

D. Alton[1,*], D. Lincoln[6,†], N. Akchurin[3], P. Birmingham[7], C. C. Chang[4], M. D. Corcoran[6], W. L. Davis[1,‡], H. R. Gustafson[5], C. Halli[4], H. Holmgren[4], P. Kasper[2], M. J. Longo[5], J. Marraffino[2], J. McPherson[3], G. Morrow[6], G. S. Mutchler[6], D. Naples[4,*], Y. Onel[3], G. P. Thomas[1], M. M. Traynor[6,§], J. W. Waters[7], M. S. Webster[7], Q. Zhu [6,‖]

(E683 COLLABORATION)

[1] *Ball State University, Muncie, IN 47306*

[2] *Fermi National Accelerator Laboratory, Batavia, IL 60510*

[3] *University of Iowa, Iowa City, IA 52242*

[4] *University of Maryland, College Park, MD 20742*

[5] *University of Michigan, Ann Arbor, MI 48109*

[6] *Rice University, Houston, TX 77005*

[7] *Vanderbilt University, Nashville, TN 37235*

(October 2, 1996)

Abstract

In Fermilab experiment E683 we have used a large solid angle calorimeter to study the production of hadronic events with large transverse energy in γp and πp collisions at center-of-mass energies from 20 to 25 GeV. We observe a sudden shift in γp event topology with increasing transverse energy, indicative of the emergence of jet dominance. This is the first observation of such a shift in event topology in fixed-target interactions. πp interactions in the

same kinematic region and under identical triggering conditions exhibit only a slight shift in event topology.

The production of particles with large momentum transverse to the beam direction in high energy hadronic interactions is well understood in terms of the hard-scattering of the constituents of hadrons, quarks and gluons, followed by the fragmentation of these constituents into "jets". Ideally a jet is a well-collimated stream of particles whose directions closely match the exiting parton and whose momenta add up approximately to the momentum of the parton.

Jets were first observed in e^+e^- interactions at center-of-mass energies (E_{CM}) ranging from 3 to 7.4 GeV. The pioneering work of Hanson et al. [1] used event topology in e^+e^- annihilations into hadrons to demonstrate the emergence of the jet signal as E_{CM} increased from 3 to 7.4 GeV. An abrupt shift in event topology with increasing E_{CM} was taken as evidence of jet production. (Note: Topological variables quantify the entire event shape, in contrast to analysis techniques which reconstruct the jets explicitly. Several different topological variables have been used, all of which yield similar results. One of these, planarity, is defined in detail below.) The reaction $e^+e^- \rightarrow$ hadrons at E_{CM} of 20 GeV and higher is totally dominated by jet production and well described by the standard model [2]. The structure observed in e^+e^- annihilations at these and higher energies is close to ideal—well-collimated jets with nothing else in the event.

Jets are also clearly seen in hadronic interactions at high energies [3]. However, even at the highest center-of-mass energies available, the bulk of the hadronic cross section consists of "soft" interactions in the non-calculable regime of low-Q^2, nonperturbative QCD. Even when jets are clearly present in hadron-hadron interactions, the event structure is less clean. The remnants of the beam and target spectators (the partons which did not participate in the hard scatter) produce additional particles not associated with the hard scattered partons, the so-called "underlying event".

A simple phenomenological model by Åkesson and Bengtsson [4] discusses the emergence of the jet signal from the background of soft processes and the underlying event. As the hardness of the interaction increases, the jet-like structure emerges and rapidly dominates, leading to an abrupt shift in event topology. One measure of the hardness of a scatter is the

total transverse energy $E_\perp$, defined as the scalar sum of $E_\perp$= E sinθ over all the particles in the detector acceptance. We therefore would expect a sudden shift in event topology with increasing total $E_\perp$, indicating the emergence and dominance of the jet signal. The $E_\perp$ at which this crossover occurs depends on E_{CM}, the detector acceptance, the relative $E_\perp$ slopes of the hard and soft cross sections, and the amount of underlying event. For large solid angle detectors and low E_{CM} the crossover may never occur.

The first attempts to observe jets in hadron-hadron collisions were at fixed-target energies with E_{CM} of 20-30 GeV. At these energies the jets are less well-collimated than at higher energies, and the overlap with spectator remnants is a more serious problem. Early attempts using limited solid angle detectors [5], although suggestive, were generally considered inconclusive due to the lack of complete information. Subsequent experiments used large solid angle detectors in order to observe the event structure more completely [6–8]. These detectors were typically large solid angle, segmented calorimeters which had full azimuthal coverage over a pseudorapidity (η) range of about two units centered at or near $\eta = 0$ in the CM. A geometrically unbiased trigger, the so-called "global" trigger was used. This trigger set a threshold on the transverse energy sum $E_\perp$, which was calculated using laboratory quantities. This trigger was intended to be sensitive to a hard-scattering process without imposing a particular structure on the event. In proton-proton collisions at E_{CM} up to 40 GeV, the sudden shift in event topology that indicates the emergence and dominance of the jet signal was not observed, even with total event $E_\perp$'s that were more than 70% of the available E_{CM}. However, at the higher E_{CM} of the ISR (E_{CM} of 45 and more clearly at E_{CM} of 60 Gev), the abrupt shift in event topology was observed and again was interpreted as clear evidence for jet production [9]. At collider energies, the jet signal is spectacular, but the bulk of the cross section is still dominated by soft processes. The emergence of the jet signal with increasing event $E_\perp$ at collider energies has been studied in detail by UA2 [10].

In Fermilab experiment E683, we have observed the production of events with large total $E_\perp$ in γp collisions using a large solid angle calorimeter with a global trigger at E_{CM} around

20 GeV. Unlike pp collisions at this energy, we observe an abrupt change in event topology with increasing $E_\perp$. For πp collisions at the same E_{CM} and under identical triggering conditions, the shift in event topology may be present but much less pronounced.

E683 was performed in Fermilab's Wide Band Photon laboratory during the 1991 fixed-target run. The beam and detector have been described in greater detail elsewhere [11]. Bremsstrahlung photons interacted in a liquid hydrogen target. After triggering and acceptance, photon energies of 50-450 GeV are observed, with a mean energy of 250 GeV. Each photon's energy is measured to 2%, exclusive of multiple bremsstrahlung effects. In addition, it was possible to configure the same beamline to accept a π^- beam. The energy of this π^- beam was chosen to have generally the same mean and range as the triggered photon spectrum.

For purposes of this analysis the primary detector used was a highly segmented calorimeter with a projective tower geometry. Each tower consisted of a structure of alternating layers of metal and scintillator. The calorimeter was segmented into four layers longitudinally and 132 towers transversely. Energy resolution was measured to be $35\%/\sqrt{E}$ for electromagnetic showers and $80\%/\sqrt{E}$ for hadronic showers. For our central beam energy of 250 GeV this detector covered an angular region of θ_{CM} of 25 degrees to 100 degrees with full azimuthal coverage, with partial azimuthal coverage out to 120 degrees. For this study, only the section of the calorimeter with full azimuthal coverage (θ_{CM} = 25 to 100 degrees, or $\Delta\eta$ =1.9) has been used. Because the beam was not monochromatic, the solid angle that the calorimeter subtended in the center-of-mass frame was not identical for all events. To ameliorate this effect, a cut restricting beam energies to the range 225 to 325 GeV was imposed. Events were triggered by taking a signal proportional to the energy observed in each tower and attenuating it by the $\sin\theta$ appropriate for that tower, thus forming the transverse energy $E_\perp$. A scalar sum of the tower's $E_\perp$ was formed using analog electronics, and two separate discriminator thresholds were applied. We refer to these two triggers as "global low" and "global high". The global low trigger was prescaled to avoid saturating the data aquisition system bandwidth. Events passing these hardware triggers were then digitized and stored

to tape. Software cuts of 5.1 GeV and 9.1 GeV (for the global low and global high trigger respectively) were imposed on the calorimeter $E_\perp$ to ensure that an event was taken in an $E_\perp$ region where the trigger was fully efficient. Both of these cuts were varied by ± 0.5 GeV in order to verify that the results were insensitive to these threshold choices. The two triggers gave consistent results and have been combined in the results presented below. Loose cuts were imposed to reject spurious events caused by muons or by breakdown in the photomultiplier tubes. In addition, a loose cut on energy conservation was required ($E_{\rm observed} < E_{\rm beam} + 75$ GeV). Target empty corrections have been made to the data in figures 2 and 4. In order to increase the number of events in the regions of poor statistics, we have not made target empty corrections to figures 1 and 3. Target empty corrections in the regions with good statistics were about 15-20% and had no qualitative effect on these distributions.

Several variables have been used to quantify the jet-like nature of hadronic events. In keeping with tradition in hadron-hadron interactions, we use planarity, which we define as follows. In the plane transverse to the beam direction we define a 2×2 matrix

$$\begin{pmatrix} \sum p_x^2 & \sum p_x p_y \\ \sum p_x p_y & \sum p_y^2 \end{pmatrix}$$

where the sum is taken over the particles in the event (or in this case all calorimeter towers) and p_x, p_y are the components of each particle's transverse momentum. One may solve the resultant eigenvalue problem for λ_1 and λ_2 and the corresponding eigenvectors $\vec{\lambda}_1$ and $\vec{\lambda}_2$. For $\lambda_1 > \lambda_2$, the eigenvector λ_1 defines the direction in the transverse plane such that $\lambda_1 = \sum p_{||}^2$, the sum of momenta parallel to that direction is maximized, and $\lambda_2 = \sum p_\perp^2$, the sum of particle momenta perpendicular to that direction is minimized. Planarity is then defined as $P = (\lambda_1 - \lambda_2)/(\lambda_1 + \lambda_2)$. For jet-like topologies, $\lambda_1 \gg \lambda_2$ and $P \to 1$. For isotropic topologies $\lambda_1 \sim \lambda_2$ and $P \to 0$. So if jet-like event topologies emerge naturally with increasing $E_\perp$, we should observe an increasing $< P >$ with increasing $E_\perp$.

Because a kinematic relationship exists between E_{CM} and the maximum $E_\perp$ achievable, we define the normalized variable $x_\perp = E_\perp / E_{CM}$. Planarity and $x_\perp$ were calculated using

the sum over calorimeter towers. Studies with the LUND Monte Carlos LUCIFER and TWISTER [12] showed that on average the detector did not significantly affect the measurement of either $x_\perp$ or planarity. The effect of the detector was to shift the planarity by an average of -2% and the $x_\perp$ by an average of -5%. We have not corrected the data for these small instrumental effects.

Figure 1a plots the distribution of planarity for three different bins of $x_\perp$ ($x_\perp < 0.34$, $0.34 < x_\perp < 0.57$, $0.57 < x_\perp$) for γp data. Figure 1b shows the same plots for πp data. All distributions are normalized to unit area. A striking feature of the γp data is the sudden shift to higher planarity with increasing $x_\perp$. The πp data may exhibit a much less pronounced shift. This point is further demonstrated in fig. 2, where the average planarity $< P >$ is plotted as a function of $x_\perp$ for both γp and πp interactions. The photon data show a sharp increase in planarity with increasing $x_\perp$, while the pion data exhibit at best a slight rise.

We can observe the same effect in another way by defining the $E_\perp$ flow as follows. The direction of the eigenvector $\vec{\lambda}_1$ (the planarity axis) defines $\Delta\phi = 0$. Each calorimeter tower is then plotted at the appropriate $\Delta\phi$, weighted by the tower $E_\perp$. A dijet event would be characterized by strong peaks at $\Delta\phi = 0$ and π, with much less energy in the region around $\Delta\phi = \pi/2$, the non-jet or underlying event region. $E_\perp$ flow has been used before [13] to study jet structure, but previously the direction of a reconstructed jet was used to define $\Delta\phi = 0$. Our approach is much more unbiased in that we are not imposing a jet-like structure on the event by requiring a jet-finding algorithm to find one or more jets.

Figure 3a shows γp $E_\perp$ flow plots for the same bins of $x_\perp$ as shown in figure 1. Figure 3b shows the same plots for πp triggers. Once again the more jet-like nature of γp interactions compared to πp interactions is apparent. In figure 3a it is interesting to note that, in going from the second to the third bin in $x_\perp$, all of the additional energy appears in the jet region ($\Delta\phi = 0$ and π), while the non-jet region ($\Delta\phi = \pi/2$) remains unchanged. The same is not true in Figure 3b.

In order to quantify the shapes of the $E_\perp$ flow plots, we take the following approach. Plots similar to those given in fig. 3 were created, each containing 30 bins in $\Delta\phi$. The area of

each plot was determined. The center six bins were taken to be representative of the non-jet fraction of the $E_\perp$. The contents of these bins, scaled up to the full $\Delta\phi$ range, was taken as the 'non-jet' area and subtracted from the total area. The remaining area was defined to be the 'jet' area. Figure 4 plots the ratio of jet area to total area as a function of $x_\perp$ for both γp and πp interactions. Once again we see a sudden shift in event topology for γp interactions which is much less apparent in the πp case.

The different behavior of γp and πp interactions is consistent with the expected difference in the parton distribution functions of pions and photons. Photons are expected to have an extremely hard parton distribution function compared to either pions or protons [14]. One would therefore expect γp interactions to have a much harder $E_\perp$ spectrum as well as less underlying event than πp interactions. For both of these reasons the hard scattering process should dominate at lower $E_\perp$ for γp interactions compared to πp interactions. We have reported earlier [15] that our π-induced events in fact do have significantly more underlying event than the γ-induced events, consistent with our observation that the pion data exhibit a much less pronounced shift in event topology.

In conclusion we have used a geometrically unbiased, large solid angle trigger to study large $E_\perp$ events in γp and πp collisions. For γp interactions we see an abrupt change in event topology as characterized as a sudden shift in planarity or $E_\perp$ flow, consistent with the dominance of jet production. A much weaker shift is observed in πp interactions under identical conditions. Previous experiments have shown that a shift in event topology is not observed in pp interactions at these energies using a similar detector and trigger. It should be emphasized that this study employed a geometrically unbiased trigger and did not employ a jet-finding algorithm of any kind. We interpret the sudden shift in event topology as the emergence and dominance of jet production in γp interactions at E_{CM} from 20 to 25 GeV. This is the first such observation of an abrupt change in event topology in fixed-target interactions. These results are consistent with the expected differences in the parton distribution functions of photons and pions.

We wish to thank all those personnel, both at Fermilab and at the participating insti-

tutions, who have contributed to this experiment. We thank the E609 collaboration for use of the detectors originally constructed for that experiment. We also wish to thank James West for help in the data analysis. This work was supported in part by the Particle Physics and Nuclear Physics Divisions of the National Science Foundation, and the Nuclear Physics and High Energy Physics Divisions of the U. S. Department of Energy.

REFERENCES

* Present address, Kansas State University, Manhattan, KS 66506

† Present address, University of Michigan, Ann Arbor, MI 48109

‡ Present address, Case Western Reserve University, Cleveland, OH 44106

§ Present address, Department of Radiation Medicine, Loma Linda, CA 92354

‖ Present address, University of California at Riverside, Riverside CA 92521

[1] G. Hanson et al., Phys. Rev. Lett. **35**, 1609 (1975); G. Hanson et al., Phys. Rev. **D26**, 991 (1982).

[2] D. Bender et al., Phys. Rev. **D31**, 984 (1985); A. Peterson et al., Phys. Rev. Lett. **55**, 1954 (1985); M. Althoff et al., Z. Phys. **C22**, 307 (1984); D. P. Barber, Phys. Lett. **108B**, 63 (1982).

[3] G. Arnison et al., Phys. Lett. **132B**, 214 (1983); J. A. Appel et al., Phys. Lett. **138B**, 430 (1984).

[4] T. Åkesson and H. U. Bengtsson, Phys. Lett. **120B**, 233 (1983).

[5] C. Bromberg et al., Phys. Rev. Lett. **38**, 1497 (1977); M. D. Corcoran et al., Phys. Rev. Lett. **41**, 9 (1978).

[6] C. De Marzo et al., Phys. Lett. **112B**, 173 (1982); C. De Marzo et al., Nuc. Phys. **B211**, 375 (1983).

[7] Arenton et al., Phys. Rev. Lett. **53**, 1988 (1984); Arenton et al, Phys. Rev. **D31**, 984 (1985).

[8] B. Brown et al., Phys. Rev. Lett. **49**, 711 (1982); C. Stewart et al., Phys. Rev **D42**, 1385 (1990).

[9] T. Åkesson et al., Phys. Lett. **118B**, 185 (1982); T. Åkesson et al., Phys. Lett. **128B**,

354 (1983).

[10] J. A. Appel et al., Phys Lett **165B**, 441 (1985).

[11] D. Adams et al., Phys. Rev. Lett. **72**, 2337 (1994); M. W. Arenton et al., Phys. Rev. **D31**, 984 (1985); K. A. Johns, M. A. Thesis, Rice University, 1983, unpublished.

[12] H. U. Bengtsson, G. Ingelman, Comput. Phys. Commun. **34**, 251 (1985); G. Ingelman, Comput. Phys. Commun. **46**, 217 (1987); G. Ingelman and A. Weigend, Comput. Phys. Commun. **46**, 241 (1987).

[13] T. Åkesson et al., Z. Phys. **C30**, 27 (1986); D. Adams et al., Phys. Rev. Lett. **72** 2337 (1994).

[14] D. W. Duke and J. F. Owens, Phys. Rev. **D22**, 2280 (1980); J. F. Owens, Phys. Rev. **D21**, 54 (1980).

[15] D. Naples et al., Phys. Rev. Lett. **72**, 2341 (1994).

Figure Captions

Figure 1. Normalized planarity distributions in bins of $x_\perp$ for (a) γp interactions and (b) πp interactions.

Figure 2. Average planarity vs. $x_\perp$ for both γp and πp interactions. Systematic errors due to the target-empty subtraction are shown as bands in the lower portion of the figure. Horizontal error bars indicate the bin sizes in $x_\perp$.

Figure 3. Transverse energy flow in bins of $x_\perp$ for (a) γp interactions and (b) πp interactions.

Figure 4. Jet area ratio (as defined in the text) vs. $x_\perp$ for both γp and πp interactions. Systematic errors due to target empty subtraction are shown as bands in the lower portion of the figure.

Figure 1

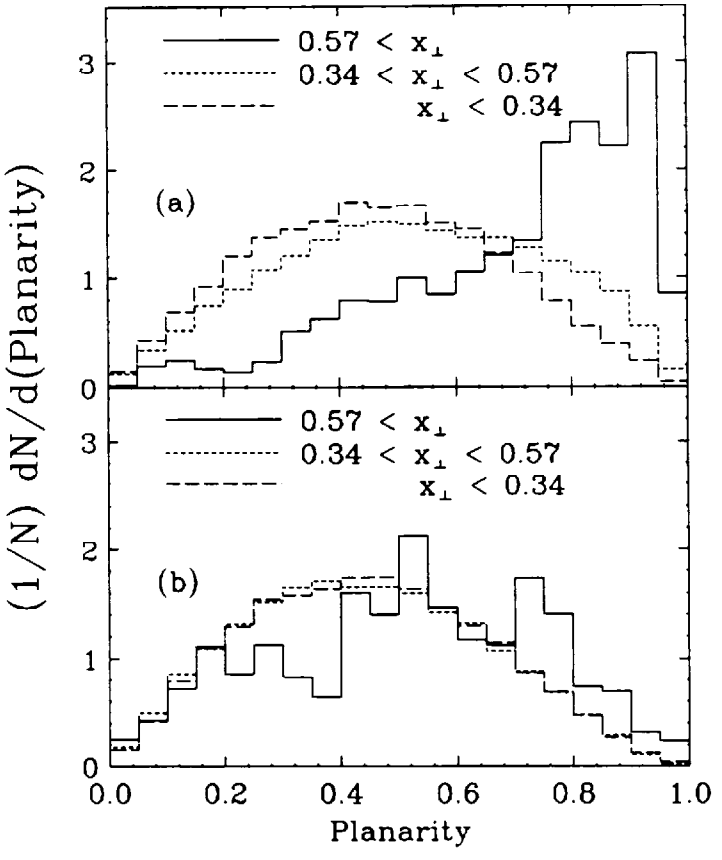
0.57 < x⊥
0.34 < x⊥ < 0.57
x⊥ < 0.34
(a)
(b)
(1/N) dN/d(Planarity)
Planarity
0.0
0.2
0.4
0.6
0.8
1.0
0
1
2
3

Figure 2

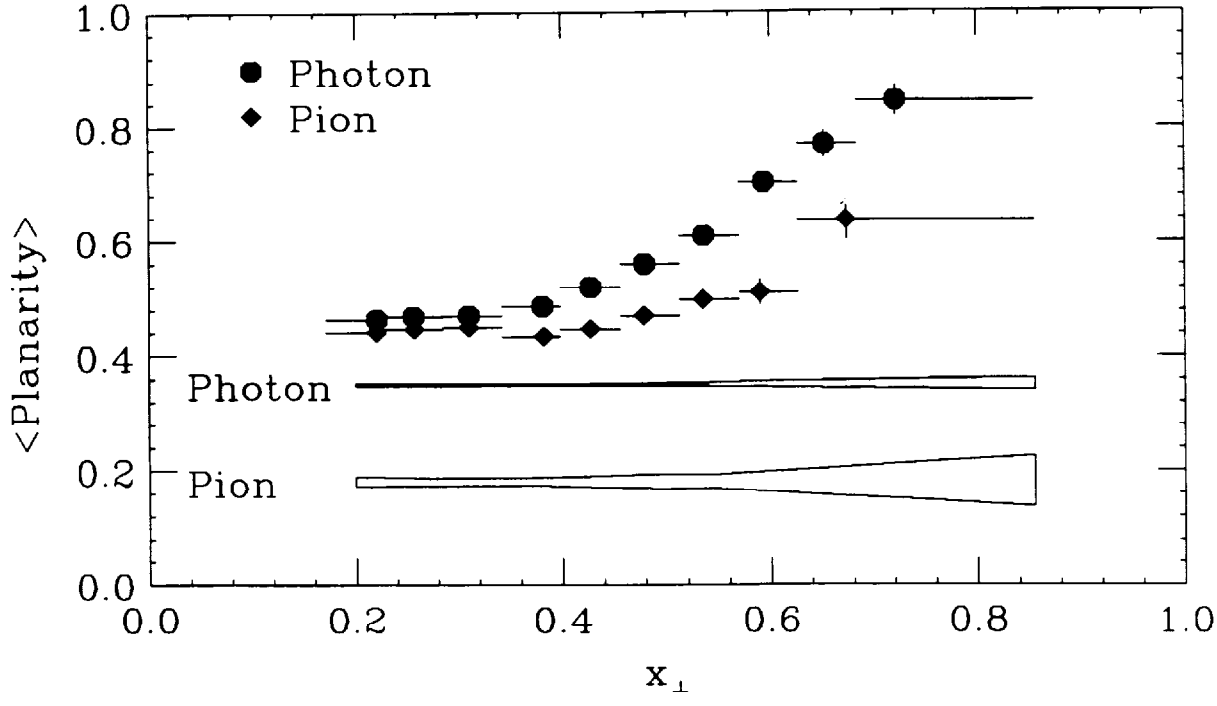

Figure 3

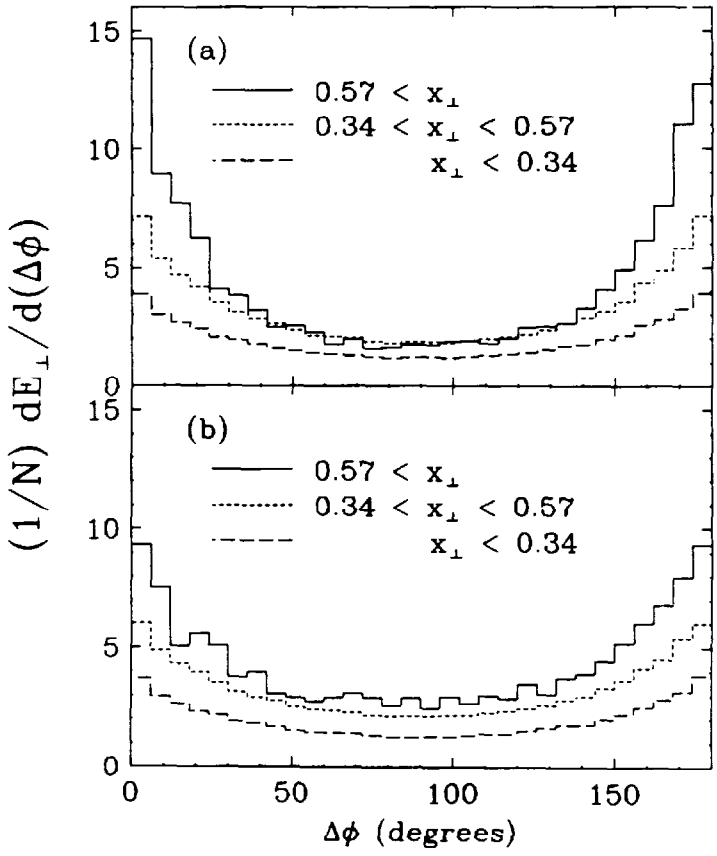
(a)
0.57 < x⊥
0.34 < x⊥ < 0.57
x⊥ < 0.34
(b)
0.57 < x⊥
0.34 < x⊥ < 0.57
x⊥ < 0.34
(1/N) dE⊥/d(Δφ)
Δφ (degrees)
0
5
10
15
50
100
150

Figure 4